

## **COMPUTATIONAL MODELLING OF MOVEMENT OF WATER SOLUBLE POLLUTANTS THROUGH SOIL**

**Akowitz, E.<sup>1</sup>, and Ampofo, J.<sup>2</sup>**

<sup>1</sup> *Mechanical Engineering Department, Cape Coast Polytechnic, Cape Coast, Ghana.*

<sup>2</sup> *Mechanical Engineering Department, KNUST, Kumasi, Ghana.*

<sup>1</sup>[ericakowitz15@gmail.com](mailto:ericakowitz15@gmail.com)

<sup>2</sup>[josh.ampofo@gmail.com](mailto:josh.ampofo@gmail.com)

### **ABSTRACT**

Most heuristic studies of hydrogeology connected with the study of water flow pattern in the ground that uses the knowledge and continuous prediction of soil permeability changes and soil porosity have been very costly; yet, no concrete comprehensive concept and results have been realized. The need for cost effectiveness in the prediction of soluble pollutants' mobility and behavior in the soil is imperative in this computational modeling era where complex problems are numerically analyzed and simulated. This paper focuses on two dimensional modelling of water soluble pollutants through soil using computational fluid dynamics (CFD) approach and adapted Navier-Stokes equations for porous flow. The model is used to simulate flow of water soluble pollutants in the soil within the laminar flow regime and to examine the dispersion of water soluble pollutants through soil layers at various Reynolds numbers. A code was developed and used to simulate the model and simulated results validated qualitatively against experimental results. The dispersion pattern of the dye used was then physically examined at various times and the results compared. It was found that all the flow patterns of the experiments were comparable to the simulated results. The lessons learned from this study, recommendations and the potential contributions to future models in pollutant mobility and dispersion in the soil and groundwater are discussed herein.

**Keywords:** computational domain; porous medium, permeability, dye solution; pollutant dispersion

### **1.0 INTRODUCTION**

Flow through and past porous media have attracted significant interest in recent years because of their importance in engineering and technology (*Alazmi & Vafai, 2001*). Researchers are still trying to understand some of the modeling aspects of flow through soils and other porous media. The porous nature of the soil enables pollutants to be conveyed from one locality to another with less resistance to movement of these pollutants. Such pollutants after an appreciable time (in months or years) would surely find their way into rivers, streams and groundwater, which serve as the major source of drinking water for most rural dwellers (*Kiptum & Ndambuki, 2012*).

Pollutants released from sources such as sewage sludge, waste liquids, among others are distributed throughout the soil system, while remaining in the soil solution as iron and organic and inorganic complexes with some remaining mobile for uptake by plants (*Amonoo-Neizer et al, 1996; Hooda et al, 1997*). Their mobility and availability depend on several factors including soil porosity, soil texture and soil pH. Changes can occur in chemical form and mobility of metal in the leachate, which are usually the result of variation in pH or reduction-oxidation (*Sims and Patrick, 1978*). This pollution of ground water may affect surface water and possibly portable water supplies depending on the nature of aquifer configuration of an area.

In Ghana, a greater percentage of waste water is illegally discharged directly into rivers and streams as well as the bare soil without treatment. Specifically, untreated sewage, poorly treated sewage, or overflow from under-capacity sewage treatment facilities can send water

bearing-diseases into rivers and oceans. A typical incidence occurred in 2009 when an overflow of a cyanide containment pond of AngloGold Ashanti, Iduapriem Mine led to cyanide leakage into nearby rivers and forests. Mining companies in Ghana sometimes illicitly dump mining waste directly into rivers or other bodies of water as a method of disposal. For instance, the Wassa community near Tarkwa Gold Mine in September, 2009 complained about cyanide spillage, as well as the release of other hazardous chemicals including arsenic, manganese, cadmium, iron, copper, and mercury, zinc and lead into water bodies through mining operation. Detailed research by the Wassa Association of Communities Affected by Mining Changes (WACAM) revealed that River Nyam in Obuasi, which is a mining community, had arsenic concentration of 13.56 as against 0.01 permissible levels required by the World Health Organization (WHO) and the Ghana Environmental Protection Agency (GEPA). A substantial proportion of these cyanide and other pollutants ultimately finds their way into poorly-treated drinking water (*Asante et al, 2007*). Huge pools of mining waste which is known as "slurry" are often stored behind containment dams. If a dam leaks or bursts, water pollution is guaranteed.

Conventionally, tracers are widely used to study the behaviour of water flow in the soil and even beyond the ground water table so as to predict and or determine the direction and velocity of ground water movement (*Papp et al, 2008*). Failures of tracer test are most commonly a result of incorrect choice of tracers, insufficient concentrations of tracers and a lack of an understanding of the hydrogeologic system being tested. Some of the most useful general tracers are bromide chloride, rhodamine WT, and various fluorocarbons.

The unfavorable drawback is that, these tracers themselves may also serve as pollutants.

However, in recent years, several analytical equations for free and porous flows have been propounded by researchers in the area of fluid mechanics, water resource management, and hydrogeology (*Hassanizadeh & Gray, 1979b; Duijn et al, 2007; Yahya & Abdulfatai, 2007*) but their analogous numerical models and simulations have not been fully realized in practical terms. Some of the prominent theoretical models are the Henry Darcy's law (1856) and the Forchheimer equation (1901) for porous flow (*Bennethum & Giorgi, 1996; Huang & Ayoub, 2008*). Interestingly, the gap between the number of theoretical equations and the corresponding numerical models continue to widen even though few models such as MODFLOW (*Mcdonald & Harbaugh, 2003*) do exist. In such models, soil and hydrogeological properties are to be determined experimentally (*Camur & Yazicigil 2001; Viman et al, 2005; Shao et al, 2013*) and subsequently used to estimate and or iterate the velocities, direction of flow and contamination levels of pollutant within porous media.

The intent of this work was to simulate water flow pattern in the soil and examine the behaviour of water soluble pollutants and to qualitatively approximate pollutant dispersion coverage area vis-à-vis its travel time and pollutant spread pattern. This would help towards the development of a sustainable model that would simulate the flow pattern of contaminated water through the soil at a cheaper cost. Such a model may be welcomed by city and town planners, borehole drillers and mining companies as it would complementarily enhance their operations in predictions and planning purposes.

## **2.0 MATERIALS AND METHOD**

### **Numerical Model**

A number of assumptions regarding the flow, characteristics of water and the porous sand medium were considered for the computational model in Figure 1. These assumptions were used in tandem with the following continuity equation (2) as well as the modified adapted

two dimensional Navier-Stokes equations (1a and 1b) that describe the flow of incompressible fluids through a porous medium (Gent, 1992; Anderson, 1995):

$$\frac{1 + C_M}{ng} \frac{\partial u_f}{\partial t} = -\frac{1}{\rho_f g} \frac{\partial p}{\partial x} - \frac{1 + C_D}{ng} \frac{\partial u_f^2}{\partial x} - \frac{1 + C_D}{ng} \frac{\partial u_f w_f}{\partial z} - C_L \frac{v}{gl_1^2} u_f - C_T \frac{l_5}{gl_4^2} u_f |u_{frep}| + \frac{a_x}{g} \dots \dots \dots (1a)$$

$$\frac{1 + C_M}{ng} \frac{\partial u_f}{\partial t} = -\frac{1}{\rho_f g} \frac{\partial p}{\partial z} - \frac{1 + C_D}{ng} \frac{\partial w_f^2}{\partial z} - \frac{1 + C_D}{ng} \frac{\partial u_f w_f}{\partial x} - C_L \frac{v}{gl_1^2} w_f - C_T \frac{l_5}{gl_4^2} w_f |w_{frep}| + \frac{a_z}{g} \dots \dots \dots (1b)$$

$$\frac{\partial u_f}{\partial x} + \frac{\partial w_f}{\partial z} = 0 \dots \dots \dots (2)$$

Let:  $k_1 = \frac{1+C_M}{ng}$ ,  $k_2 = \frac{1+C_D}{n^2g}$ ,  $k_3 = \frac{1}{\rho_f g}$ ,  $k_4 = C_L \frac{v}{gl_1^2}$ ,  $k_5 = \frac{1}{g}$ ,  $k_6 = C_T \frac{l_5}{gl_4^2}$ , and  $v = \frac{\mu}{\rho_f}$

And Let:  $K_x = -k_4 u_f$  and  $K_z = -k_4 w_f$

Insisting on assumptions about turbulent flow and inertia forces cancel the turbulence term and the inertia terms, yielding the following equations:

$$k_6 = C_T \frac{l_5}{gl_4^2} \xrightarrow{\text{yields}} 0 \text{ and } k_5 = \frac{1}{g} \xrightarrow{\text{yields}} 0$$

$$k_1 \frac{\partial u_f}{\partial t} = -k_3 \frac{\partial p}{\partial x} - k_2 \left( \frac{\partial u_f^2}{\partial x} + \frac{\partial u_f w_f}{\partial z} \right) + K_x \dots \dots \dots (3a)$$

$$k_1 \frac{\partial w_f}{\partial t} = -k_3 \frac{\partial p}{\partial z} - k_2 \left( \frac{\partial w_f^2}{\partial z} + \frac{\partial u_f w_f}{\partial x} \right) + K_z \dots \dots \dots (3b)$$

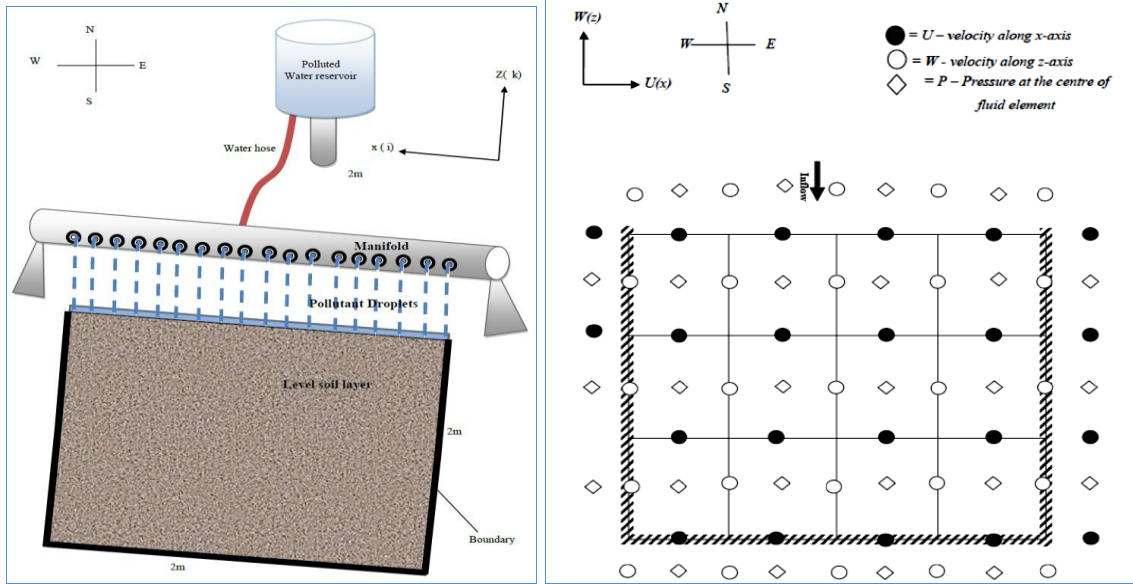
The simplified equations representing equations 2, 3a and 3b are:

$$U_x + W_z = 0 \dots \dots \dots (4)$$

$$k_a U_t = -k_p p_x - k_c (U^2)_x - k_c (UW)_z - k_l u_f \dots \dots \dots (5a)$$

$$k_a W_t = -k_p p_z - k_c (UW)_x - k_c (W^2)_z - k_l w_f \dots \dots \dots (5b)$$

Advective = - Pressure - Convective - Constant (Laminar Resistance)



(a) (b)

Figure 1: Computational model (a) Schematic setup (b) Staggered grid

**Numerical Solution**

The equation (2) is solved by generating a system of new velocities after every n+1 time step for all grid points as:

$$U^{n+1} = U^n - (k_p/k_a)\Delta t[\nabla(P^{n+1})] \dots \dots \dots (6)$$

The continuity equation (1) may be analogously treated as a stream function  $Q^n$  as follows:

$$\text{Compute } F^n = (W^n)_x - (U^n) \dots \dots \dots (7a)$$

$$\text{And } -\Delta Q^n = -F^n \dots \dots \dots (7b)$$

The concentrations of pollutants were computed once the velocity fields have been determined. The equation for the mobility of heavy metals in a porous medium like soil is

$$\text{given by } C = e^{\frac{1}{(1+\frac{k_{dc}\rho_b}{\theta})}t} - e^{\frac{v_x x}{D_L}} \text{ (after DeCapio, 2003).} \dots \dots \dots (8)$$

The Equation 8 above was transformed into a two dimensional form as follows:

$$C_u = e^{\frac{1}{(1+\frac{k_{dc}\rho_b}{n})}t} - e^{\frac{u}{D_L}x} \dots \dots \dots (9a)$$

$$\text{and } C_w = e^{\frac{1}{(1+\frac{k_{dc}\rho_b}{n})}t} - e^{\frac{w}{D_L}z} \dots \dots \dots (9b)$$

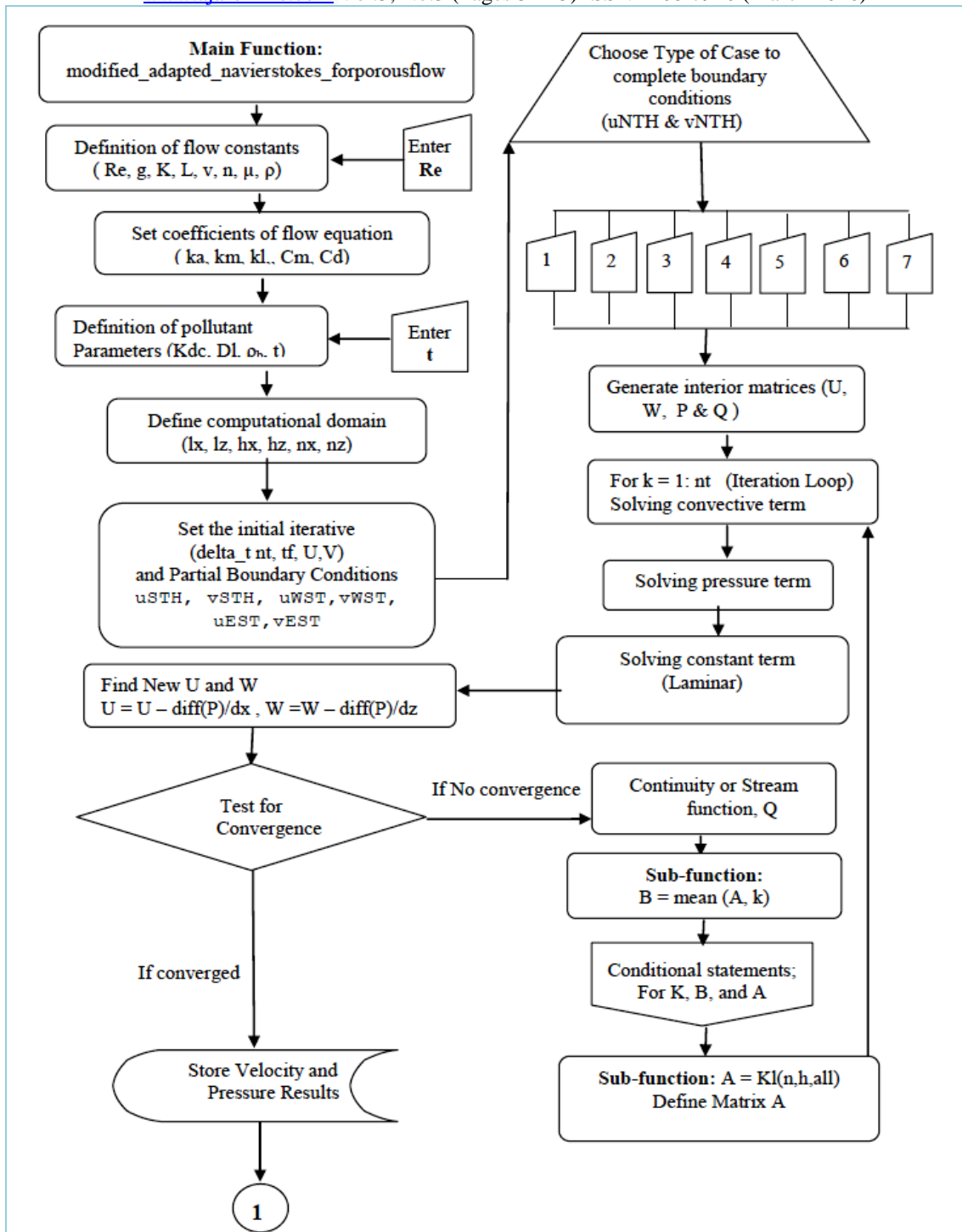


Figure 2a: Flow chart for the numerical simulation (Continuation on next page)

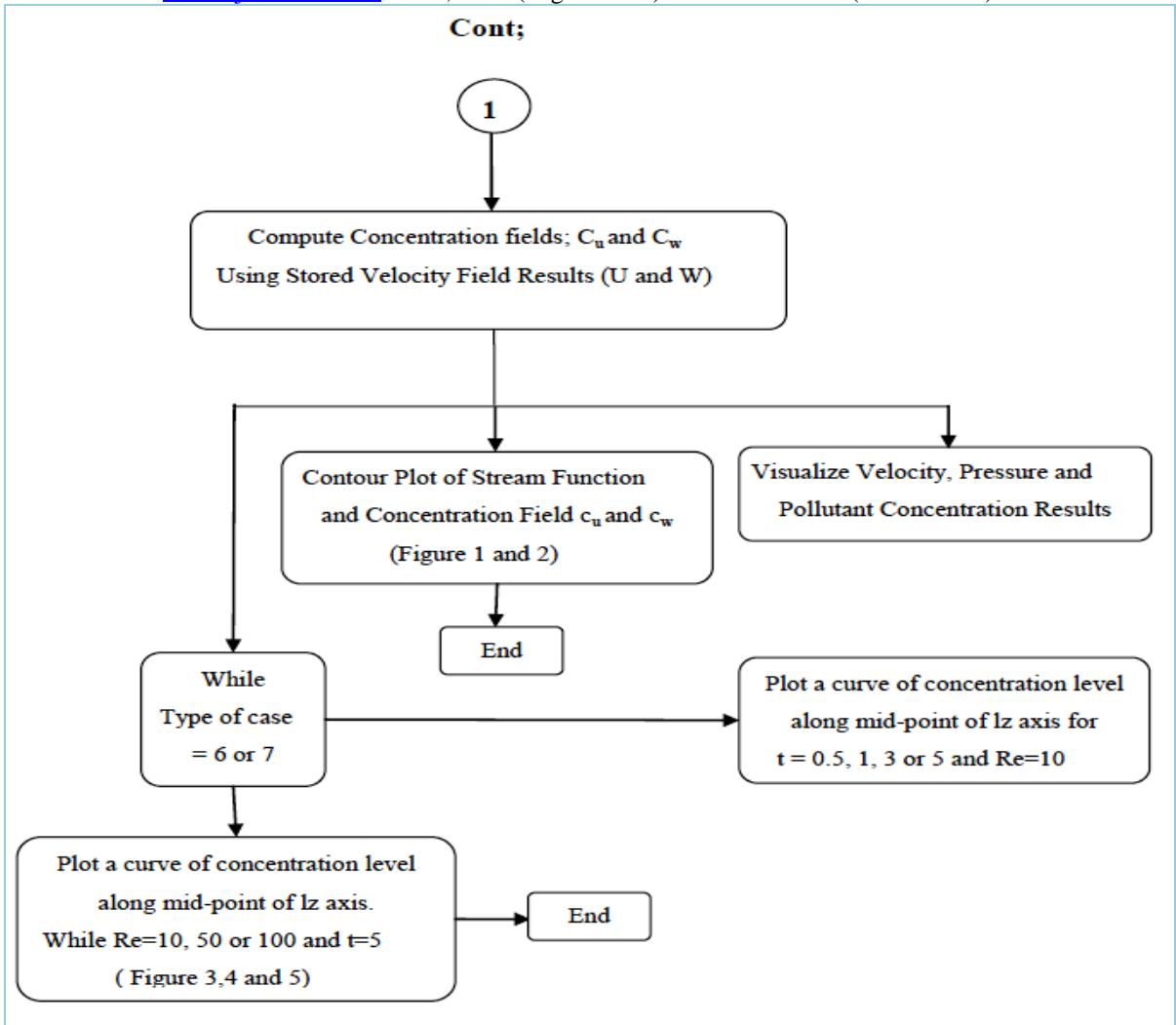


Figure 2b: Flow chart for the numerical simulation (extension)

In the computational domain, the concentration fields would behave in the following form:

$$C_u^{i+0.5} = e^{\frac{1}{\left(1+\frac{k_{dc}\rho b}{n}\right)^t}} - e^{\frac{u^{i+0.5}}{D_L}dx} \dots \dots \dots (10a)$$

$$\text{and } C_w^{k+0.5} = e^{\frac{1}{\left(1+\frac{k_{dc}\rho b}{n}\right)^t}} - e^{\frac{w^{k+0.5}}{D_L}dz} \dots \dots \dots (10b)$$

The flow chart for the numerical simulation in Matlab program is explicitly shown in Figures 2a and 2b. The flow velocity in terms of Reynolds number and the assumed travel time of pollutants, as well as preset boundary conditions (numbered 1-7 in flow chart) are specified. A Matlab code was developed and used to solve the Equation 10a and 10b for seven different boundary conditions and at varied dispersion times as well as Reynolds numbers. The program runs through a series of iteration until the solution converges.



Once convergence is arrived, the computation ends, simulation results are graphically generated and the results are captured for analysis. The code is flexible enough to be massaged in the M-file of Matlab for different porous media and run to give parallel results.

### **Experimental Model and Setup**

Analogous physical model was built to corroborate the numerical results by way of qualitative comparison. The setup (*Figure 3*) was simple and comprised a two square meter wooden wall, labeled as northern, southern, eastern and western boundaries. A water-proof rubber carpet was placed beneath the two square metre wooden wall and filled with a three centimeter depth of fine sand (*plastering sand*) evenly and horizontally spread on the carpet within the square walls. The boundaries (*wooden walls*) were secured with eight pegs to the level ground. A two metre long, one inch diameter PVC pipe with linear perforations on it and both ends closed and a water hose connected to the reservoir and PVC pipe was used to convey dye solution (*soluble pollutant*) from the dye solution reservoir. The pollutant reservoir and the PVC pipe were placed at the same height of 30cm above the fine sand.



*Figure 3: Experimental setup of soluble pollutant flow through fine sand.*

There were assumptions made with regard to the experimental setup. One of them has to do with the thickness of sand used. The thickness of fine sand within the 2-m square wooden wall is assumed to be of unit depth to conform with 2D flow. The other has to do with the likelihood of distortion in the orientation of particles during flow. Here, the natural orientation of the sand particles as well as its associated porosity and permeability is assumed to remain unchanged. Finally, the pressure with which the dye enters the sand is assumed to be that of atmospheric pressure. Concurrently, the flow of the dye through the sand is assumed to be purely laminar with low Reynolds numbers throughout the experiment.

### **Determination of Coefficient of Permeability**

The falling head permeability test was used to determine the permeability of fine sand. At the Geotechnical Engineering Laboratory, the reamer and the proctor mould setup was used

to approximate the coefficient of permeability of fine sand. Using the Darcy’s law, the permeability is computed as follows:

$$k = 2.3 \frac{al}{At_1} \log \frac{h_0}{h_1} \dots\dots\dots(11)$$

The average permeability,  $k$  for fine sand for three different results of  $k$  is found as;

$$k = \frac{k_{(1)}+k_{(2)}+k_{(3)}}{3} \dots\dots\dots(12)$$

$$k = 5.8157 \times 10^{-6} cm/s$$

Then the absolute or intrinsic permeability,  $K$  is given by;  $K = k \times \frac{\mu}{\gamma} \dots\dots\dots(13)$

*This gives absolute permeabilty,  $K = 5.9283 \times 10^{-14} m^2$ .*

Where; *specific weight of water,  $\gamma = \frac{9.81kN}{m^3}$  and Viscosity,  $\mu = 10^{-3} kg/ms$*

**3.0 RESULTS AND DISCUSSION**

The numerical and experimental results obtained from the two analogous models are shown in Figures 5 and 6. A close examination revealed that each complementary pair of results was similar by qualitative comparison. In Figure 5a, the pollutant was placed along the whole length of the northern boundary. It is observed that the pollutant dispersed in a U-shaped wave form as the concentration levels fall gently from the source to the sink. It is very interesting to visualize that as the pollutant source was further moved along the northern boundary at about 40% lengthwise way from the western boundary, a true eccentric wave form dispersion of the pollutant was obtained. This is evident from Figure 5b where the eccentric wave of concentration profile declined gently from the source to the sink. A more unique development was considered where the pollutant was placed within the computational domain 50% lengthwise by 20% breadth as illustrated in Figure 6. As clearly observed, a true concentric wave form dispersion of the pollutant is exhibited. The concentration of the pollutant, once again, decreases from the source (*with pink colour*) to the sink (*with blue colour*) as indicated by the colour bar.

The complementary experimental results shown at the right side of each of the three simulations in Figures 5a, 5b and 6 are photographs captured during the experiment at the fifth hour, respectively. It could be observed that each of the experimental results fully corroborate that of the counterpart numerical results discussed. This is because the flow pattern and configuration of the simulated results and experimental results are very similar; hence, the two results are qualitatively comparable.



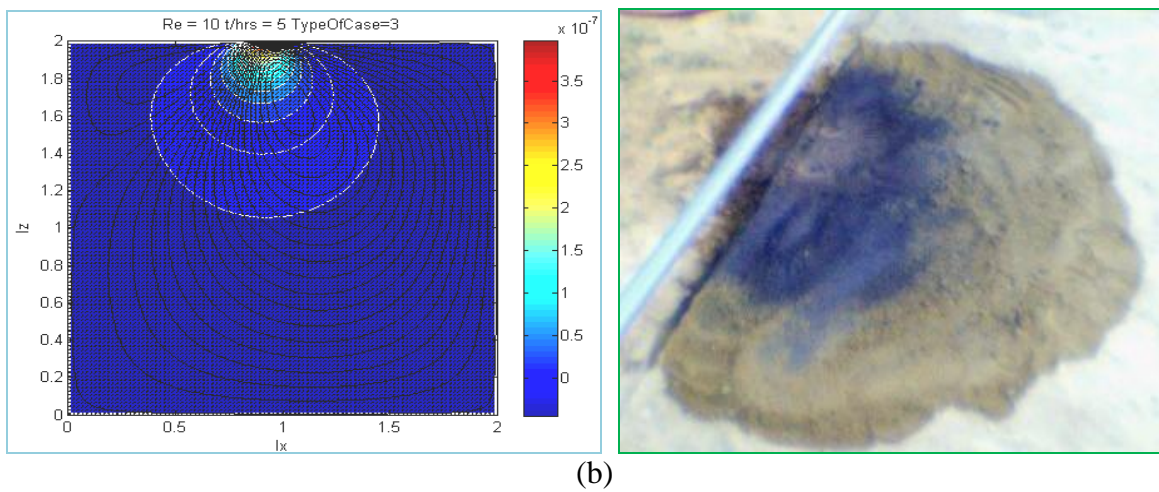
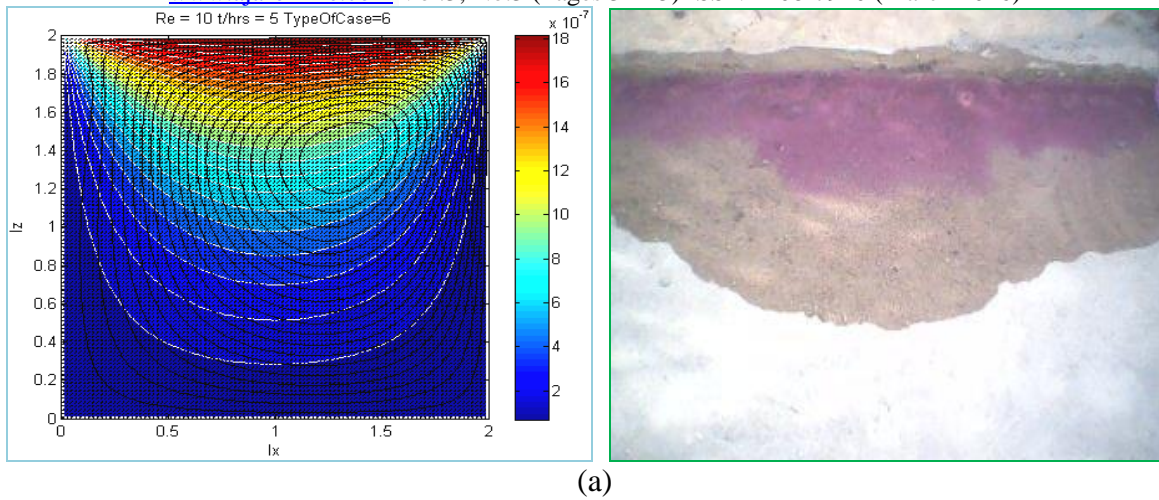
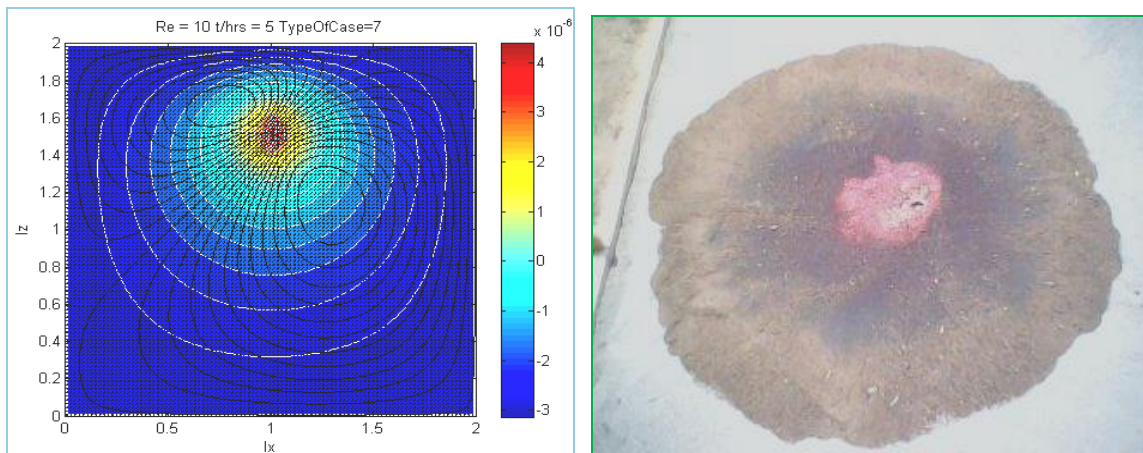


Figure 5: Numerical(left) and Experimental(right) results of pollutant dispersions at:  
(a) pollutant along northern boundary and (b) midpoint of northern boundary



**Factors Affecting Pollutant Dispersion**

Apart from source concentration levels and velocity of flow or the Reynolds number, another parameter that has influence on the rate of pollutant travel in a computational field is time. From figures 7a and 7b illustrated below, it is evident that the gradients of concentration levels ( $C_g$ ) determined have a constant concentration rate of distribution at times 1 hour and 5 hours and for both cases 6 and 7. The longer the time interval, the higher the concentration levels along the midpoint of  $l_z$  as more moles of the pollutant are able to disperse and travel to the midfield of the computational domain. In both cases considered, the gradients ( $C_g$ ) of the various curves remain constant with  $C_g = -1.725 \times 10^{-11} \text{ kmol/m}^3$  and  $C_g = -6.192 \times 10^{-11} \text{ kmol/m}^3$  for case 6 and 7, respectively at all times. The implication is that the rate of pollutant dispersion depends on the pollutant travel time as the higher the pollutant travel time, the higher the rise in concentration levels of a given monitoring point. Moreover, the pattern of pollutant dispersion depends on the source of the pollutant and its boundary conditions. This is because unique dispersion patterns were recorded for cases 6 and 7 at all time intervals irrespective of the pollutant moles dispersed.

In addition, a section of the results generated from the Matlab codes confirmed that the higher the Reynolds number for the same quantum of pollutant concentration at fixed source, the more swift, irregular and haphazard the dispersion of that pollutant.

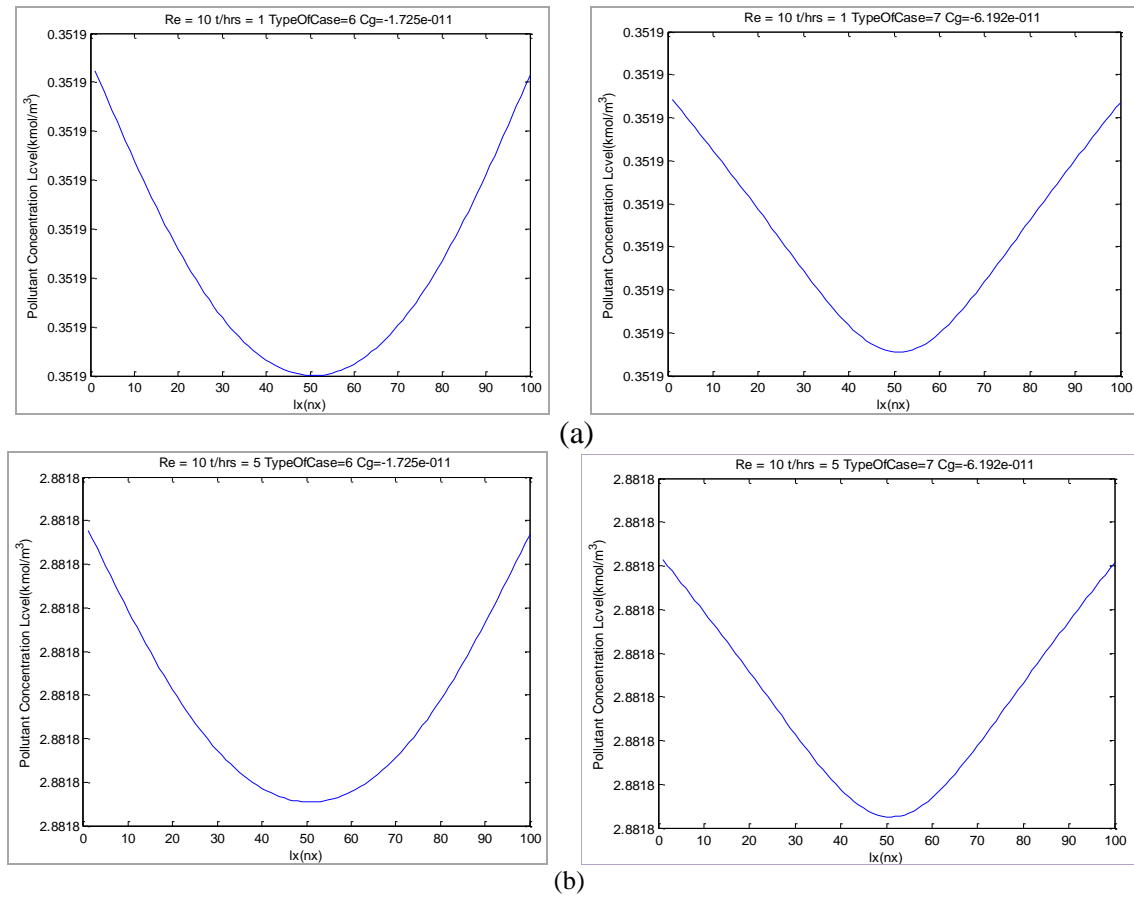


Figure 7: Concentration of dispersed pollutant for two different locations of plummets after:  
 (a) One hour pollutant leakage (b) Five hour pollutant leakage

#### **4.0 CONCLUSION AND RECOMMENDATIONS**

Matlab code for simulating water soluble pollutants through soil has been developed and numerical results validated against experimental results. The code is fundamentally dependent on a modified form of the adapted Navier-Stokes equation for porous flow. It is used to simulate how water soluble pollutants manoeuvre their way through homogenous soil and any other homogeneous porous media. There exists a fairly consistent relation between the flow pattern, pollutant dispersion and the flow variables. This is more comprehensive when the concentration levels along the mid-point of the computational domain were determined and analyzed at varying Reynolds numbers and times. The code was validated qualitatively using an experimental set-up performed by physically monitoring of the flow of a dye from three different sources within a two square metre by three centimetre depth of fine sand spread over a water proof carpet on a level ground. The distribution and dispersion pattern of the dye used was then physically examined at various times as simulated in the code and results compared. It was found that the concentration of the dye qualitatively decreased away from the source. This coincided with the physical analysis and observation of the dye configuration obtained at the end of all the three experiments. It is postulated that water soluble pollutants travel uniformly through homogenous soil from a source to a sink as their concentration level from the source to the fixed point under monitoring also increases qualitatively with time. It has become clear that the higher the Reynolds number (velocity) of the flow, the higher the rate of pollutant distribution from the source to the fixed point(s) being monitored. Additionally, pollutants may disperse in conical, U, eccentric and concentric shapes from a source to sink depending on boundary conditions. It is suggested that that there exists a very good level of agreement between the experimental and numerical results obtained.

Notwithstanding the fact that the model developed could be considered to be a good representation of the phenomenon of mobility of pollutants in the soil, several inputs are required by future environmental researchers to ensure the development of a more adaptable code. Future codes should be extended to include obstacle or non-permeable and non-homogenous medium in the computational domain so that pollution around impermeable obstacles such as hardened rocks, concrete wall, moulds or metallic moulds and confinements could be modeled. A wide variety of experimental models with different soil types should be built and results harmonized with simulated results for upgrading of code. Moreso, reverse coding could be developed for tracing pollution sources, especially soluble pollutants found in underground water.

#### **REFERENCES**

- Alazmi, B., & Vafai, K. (2001). Analysis of fluid flow and heat transfer interfacial conditions between a porous medium and a fluid layer. *International Journal of Heat and Mass Transfer*, 44(9), 1735-1749.
- Amonoo-Neizer, E. H., Nyamah, D., & Bakiamoh, S. B. (1996). Mercury and arsenic pollution in soil and biological samples around the mining town of Obuasi, Ghana. *Water, Air, and Soil Pollution*, 91(3-4), 363-373.
- Anderson, J. D. J. (1995). *Computational Fluid Dynamics: The basics with applications*. New York, McGraw-Hill Inc. ISBN 007-0015-2
- Asante, K. A., Agusa, T., Subramanian, A., Ansa-Asare, O. D., Biney, C. A., & Tanabe, S. (2007). Contamination status of arsenic and other trace elements in drinking water and

- residents from Tarkwa, a historic mining township in Ghana. *Chemosphere*, 66(8), 1513-1522.
- Bennethum, S. L. and Giorgi, T. (1996). Generalized Forchheimer Equation for Two-Phase Based on Hybrid Mixture Theory. [<http://ccm.ucdenver.edu/reports/rep092.pdf>], (accessed 2016, February 15).
- Camur, M. Z., & Yazicigil, H. A. S. A. N. (2001). Experimental determination of hydrodynamic dispersion coefficients for heavy metals using compacted clay. *IAHS PUBLICATION*, 283-286.
- DeCapiro, V. (2003). Lead Sorption on Goethite Coated Silica Sand Columns. *Environmental Engineering Science, Washington, USA*, 3-13.
- Duijn, V.C. J., Eichel, H., Helmig, R., & Pop, I. S. (2007). Effective equations for two-phase flow in porous media: the effect of trapping on the microscale. *Transport in porous media*, 69(3), 411-428.
- Gent, V. M. R. A. (1992). Formulae to describe porous flow. Communications on hydraulic and geotechnical engineering report. Delft University of Technology, Report No. 92-2. ISSN 0169658.
- Hassanzadeh, M., & Gray, W. G. (1979b). General conservation equations for multi-phase systems: 2. Mass, momenta, energy, and entropy equations. *Advances in Water Resources*, 2, 191-203.
- Hooda, P. S., McNulty, D., Alloway, B. J., & Aitken, M. N. (1997). Plant availability of heavy metals in soils previously amended with heavy applications of sewage sludge. *Journal of the Science of Food and Agriculture*, 73(4), 446-454.
- Huang, H., & Ayoub, J. A. (2008). Applicability of the Forchheimer equation for non-Darcy flow in porous media. *SPE Journal*, 13(01), 112-122.
- Kiptum, C. K., & Ndambuki, J. M. (2012). Well water contamination by pit latrines: a case study of Langas. *International Journal of Water Resources and Environmental Engineering*, 4(2), 35-43.
- McDonald, M. G., & Harbaugh, A. W. (2003). The history of MODFLOW. *Ground water*, 41(2), 280-283
- Papp, B., Deak, F., Horvath, A., Kiss, A., Rajnai, G., & Szabo, C. (2008). A new method for the determination of geophysical parameters by radon concentration measurements in bore-hole. *Journal of environmental radioactivity*, 99(11), 1731-1735.
- Shao, A. J., Chen, J. H., & Huang, Y. (2013, March). Experimental Determination of Coefficient of Soil Hydrodynamic Dispersion. In *Advanced Materials Research* (Vol. 671, pp. 380-383). Trans Tech Publications.
- Sims, J. L., & Patrick, W. H. (1978). The distribution of micronutrient cations in soil under conditions of varying redox potential and pH. *Soil Science Society of America Journal*, 42(2), 258-262.
- Viman, V., Cozmata, L. M., Cozmata, A. M., Vatca, G., Varga, C., & Oprea, G. (2005). Mathematical Modelling of Pollutants' Dispersion in Soil I. Case Study of Copper Dispersion. *American Journal of Environmental Sciences*, 1(2), 126-129.
- Yahya, M. D., & Abdulfatai, J. (2007). Mathematical modelling and simulation of mobility of heavy metals in soil contaminated with sewage sludge. *Leonardo Electronic journal of practices and technologies*, 6(10), 157-168.